XXI IMEKO World Congress "Measurement in Research and Industry"
August 30 – September 4, 2015, Prague, Czech Republic

ROTOR BAR PRE-FAULT DETECTION IN THE SQUIRREL CAGE INDUCTION MOTORS

Antonino Oscar Di Tommaso, Rosario Miceli, Ciro Spataro

Department of Energy, Information Engineering and Mathematical Models
University of Palermo, Italy, ciro.spataro@unipa.it

Abstract – The paper deals with a diagnosis technique to detect and monitor incipient faults in the rotor bars of squirrel gage induction motors. The failure mode analysis is performed monitoring the motor axial vibrations. To accomplish the task, the authors present a mathematical model that allows relating the occurrence and the severity of the faults to the presence and the magnitude of some frequency components of the axial vibration spectrum. To validate the proposed approach, the results obtained by applying the mathematical model are compared with the ones obtained by experimental tests done on both healthy and faulty motors.

Keywords: fault detection, squirrel cage motors, vibration analysis,

1. INTRODUCTION

A comprehensive analysis of the failure modes in the induction motors reveals that about the 15 % of the motor faults is due to rotor bar cracks or breaks [1].

The main and traditional diagnostic techniques to detect broken rotor bars are based on the frequency analysis of the stator currents and on the statement that no current flows in a broken bar [2-3]. For squirrel cage motors, mainly the bigger ones, as long as the contact impedance between the rotor bars and iron core is small or the copper bars are directly inserted into the laminated iron slots, the broken bars is no longer a physical condition ensuring an open circuit and interbars or cross-path currents can flow [4-5]. Consequently, these currents interact with the radial component of the air-gap magnetic field, compensate the rotor asymmetry caused by rotor bar damage and reduce the amplitudes of rotor fault components in stator currents. In this case, the diagnosis techniques based on the harmonic analysis of the stator currents could fail, since the fault related components are too small to be detected.

For this reasons, various diagnostic techniques based on the analysis of the motor axial and radial vibrations were proposed [6-7].

These techniques are based on the assumption that the rotor bar is completely broken and, therefore, no current is flowing through it. However, it would be very useful to detect also a partial crack of the bars, which, even if does not jeopardise the motor functions, often evolves toward a complete interruption. With this aim, in this paper, we propose a diagnostic procedure to detect incipient bar faults in squirrel cage induction motors.

To accomplish the task, we generalize and extend a mathematical model of the motor already presented in a previous work [8]. The new model is able to associate the occurrence and the severity of the faults to the presence and the magnitude of some frequency components of the axial vibration spectrum and, therefore, to detect both the pre-fault and the fault conditions on rotor bars. Finally, the proposed approach is validated by comparing the results obtained using the mathematical model with the ones acquired from experimental tests.

2. MATHEMATICAL MODEL

In [8], the authors presented a mathematical model for the detection of a broken bar in squirrel cage induction motors. The mathematical model, which considers the spatial distribution of the magneto motive force permits to evaluate the axial force frequency spectrum.

In this work, that mathematical model is extended to the more general case of a cracked rotor bar, being the broken bar a limit case of the cracked one.

The generalized mathematical model was developed assuming that the crack of the bar can be modelled as an interruption of part of the cross section of the bar itself.

Fig.1 shows the cracked bar (B) and two adjacent healthy bars (A and C); $I_T/2\text{-}I_b(x)$ is the current that flows in the healthy bar and $dI_b(x)$ is the elementary current flowing from the elementary surface of the cracked bar to the healthy ones. h is the amplitude of the cracked or broken part of the bar and l its total length.

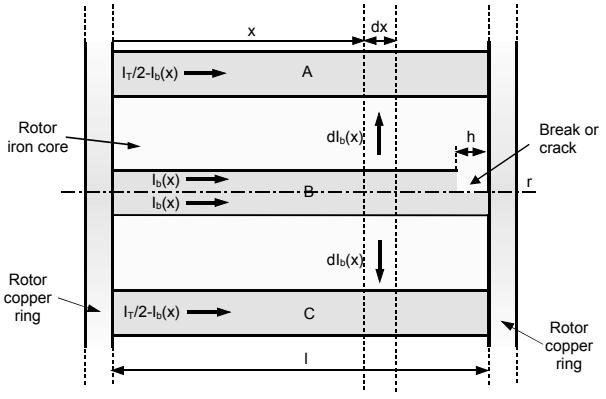

Fig. 1. Schematic of the cracked rotor bar

Moreover, it was supposed that the current $I_b(x)$ flowing at the end of the bar in which the pre-fault occurs (B) is not equal to zero, but is equal to I_n/k, being I_n the current flowing in half of the bar when it is healthy and k a variable that depends both on the cross section of the crack and on the contact impedance between the rotor bar and iron core (this contact impedance remain substantially constant with the entity of the bar crack).

For sake of simplicity and without any loss of generality, we hypothesized that the current in the cracked section varies linearly with the cross section of the crack.

To assess the axial force it is necessary to calculate both the interbar transverse currents and the radial component of the airgap magnetic field. More exactly the axial force acting on the rotor is calculated as the cross product between the rotor interbar current time harmonics and the stator magneto motive force spatial harmonics.

The basic hypothesis to determine the equations of the model are [6]:

- the interbar currents flow only between two adjacent bars;
- the voltages induced in a cracked bar and the two adjacent ones are equal and in phase with one another;
- the interbar impedance is mostly resistive at the pertinent frequencies;
- the impedance of the end-ring portion between adjacent bars is negligible;
- the amplitude of the cracked or broken part of the bar is negligible with respect to the length of the bar;
- the current flowing out from the lower bar surface to the core is neglected.

With these assumptions and using the symbols listed in Table 1, the amplitude of the q-th current harmonic that flows in each rotor bar in healthy working conditions is given by:

$$I_{bq} = -\frac{2\sqrt{2} l D m I_1 N_1 \mu_0 s_{q_b} f}{p q_b{}^2 l_g Z_{bq}} K_{mq_b} K_{eq_b} K_{cq_b} \qquad (1)$$

and the q-th spatial harmonic of the stator mmf can be calculate as:

$$B_q = \sqrt{2} \frac{m I_1 N_1 \mu_0}{\pi p q_a l_g} K_{mq_a} K_{eq_a} K_{cq_a} \qquad (2)$$

The analytical formula of the axial force, which takes into account the crack by introducing the variable k, is given by:

$$F = \sum_{q_a=2mg+1} \sum_{q_b=2mg+1} \frac{B_q \eta I_{bq} \lambda}{k q_a \theta_s} \left[1 - \frac{1}{\cosh(\lambda)}\right] \cdot$$

$$\cdot \left\{\cos\left[\left(2-(q_a+q_b)+(q_a+q_b)s\right)\omega t - q_a\theta_{ref} - q_a\theta_s - \varphi_{bq_b}\right] + \right. \qquad (3)$$

$$\left. + \cos\left[\left((-q_a+q_b)+(q_a-q_b)s\right)\omega t - q_a\theta_{ref} - q_a\theta_s + \varphi_{bq_b}\right]\right\}$$

where

$$\lambda = \sqrt{3\left|\frac{Z_{bq_b}}{Z_{cq_b}}\right|} \cong \sqrt{3\left|\frac{Z_{bq_b}}{R_c}\right|} \qquad (4)$$

$$\eta = \cos(q_a\theta_s) - 1 \qquad (5)$$

$$K_{cq_a} = \frac{sin\left(q_a \frac{\pi}{2}\frac{c}{\tau}\right)}{q_a \frac{\pi}{2}\frac{c}{\tau}} \qquad (6)$$

$$K_{cq_b} = \frac{sin\left(q_b \frac{\pi}{2}\frac{c}{\tau}\right)}{q_b \frac{\pi}{2}\frac{c}{\tau}} \qquad (7)$$

$$g = -\infty, ..., -2, -1, 0, 1, 2, ..., +\infty \qquad (8)$$

Table 1. List of used symbols

q_a, q_b	harmonic orders
B_q	q-th harmonic stator magnetic field in rotor coordinates
μ_0	permeability of vacuum
ω	electrical angular supply frequency
f	supply frequency
I_1	stator phase current (rms)
t	time coordinate
I_{bq}	q-th harmonic bar current
K_{eq}	winding factor for q-th harmonic
K_{mq}	pole pitch shortening factor for q-th harmonic
K_{cq}	coil width factor for q-th harmonic
l	axial length of the rotor
lg	air gap length
m	number of stator phases
N_1	number of stator turns per coil
p	number of pole pairs
τ	pole pitch
c	coil width
D	diameter of stator bore
Z_{cq}	impedance of the interbar rotor iron core at q-th harmonic
Rc	contact resistance between bar and rotor core
s	slip
s_q	harmonic slip
Z_{bq}	q-th harmonic bar impedance
φ_{bq}	q-th harmonic bar current phase
θ_s	rotor interbar angle
θ_{ref}	rotor reference coordinate

Carrying out the Fourier transform of the axial force, the axial force frequency components, due to interbar currents, are obtained. We carried out several simulations using the above-mentioned model under various loads and with various degrees of fault. The analysis of the simulation results show that when a pre-fault condition occurs, several components arise in the axial force frequency spectrum.

This components are located in the proximity of the frequencies $6if$ where i = 1,2,3 …… In particular, three frequency components appear below each above mentioned harmonic of the supply frequency.

The frequencies of these components are function of the motor slip, and, therefore of the motor load; the amplitudes of these components depend mainly on the entity of the crack of the rotor bar, but also on the slip.

3. EXPERIMENTAL VALIDATION

In order to validate the generalized mathematical model, we set up a test bench, whose components are:

- three squirrel cage induction motor, whose parameters are reported in Table 2;
- a 3-phase 30 kVA 0-380 V autotransformer to supply the motor
- a 7,83 kW four quadrants dc electrical drive to create the mechanical load;
- a piezoelectric accelerometer Brüel & Kjær, model 4507 B 005, mounted on the shield in order to measure the axial acceleration;
- a signal-conditioning network Brüel & Kjær, model NEXUS 2693;
- a four channels YOKOGAWA DL 1740 oscilloscope.

Table 2. Induction motor characteristics and parameters

Rated power	5,5 kW
Rated voltage	400 V
Rated current	13 A
Rated frequency	50 Hz
Rated speed	2870 rpm
Power factor	0,88
Diameter of stator bore	110 mm
Stator slot opening	3 mm
Stator slot pitch	11 mm
Coil pitch	13/18
Coil diameter	4 mm
Number of coil conductors	21
Conductor diameter (two in parallel)	0,95 mm
Air gap length	0,5 mm
Number of stator slots	36
Type of stator winding	Single layer lap
Rotor diameter	110 mm
Axial length of the rotor	90 mm
Max. Rotor slot diameter	5 mm
Rotor slot pitch	11 mm
Number of rotor slots	30

The validation of the model is based on the comparison of the axial measured vibration spectra and the ones obtained by applying the mathematical model at different bar crack conditions.

Before carrying out this comparison, it is necessary to characterize the mechanical behaviour of the motor, acquiring the mechanical transfer function, which links the axial forces acting on the rotor with the axial vibrations of the motor.

With this aim, a bump test was carried out on the motor under test, by using a bump hammer to strike the motor with a force pulse.

The resultant input pulse and the relative output waveform were acquired and then processed with the MATLAB® identification toolbox software. The algorithm used is ARMAX (Auto Regressive Moving Average with eXternal input). The input and output waveforms and the estimated impulse response spectrum are reported respectively in Fig. 2 and Fig. 3. A resonance peak was observed in stator free axial vibration spectrum at 500 Hz and some others above 1000 Hz frequency. These resonant peaks make difficult the identification of the axial vibration harmonics located above 1000 Hz. For these reasons only the axial vibration spectrum till $6f$ has been considered.

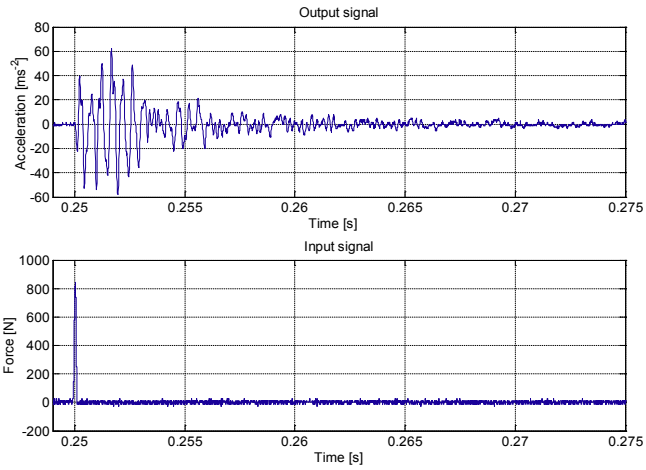

Fig. 2. Output and input registrations of the bump test.

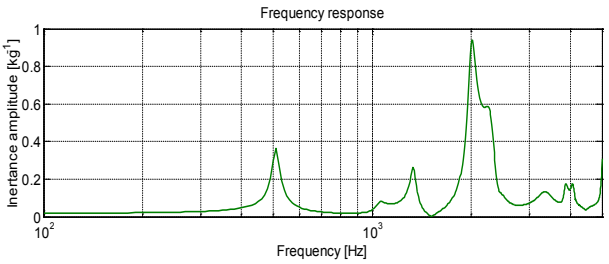

Fig. 3. Spectral response of the mechanical system.

In a second step, we carried out various tests at different loads both in healthy, cracked and broken bar conditions (two motors were damaged on purpose). The axial vibration signals were sampled at 5000 S/s rate with time windows of 10 s.

By comparison of all the measured axial vibration spectra with the simulated ones, obtained by applying the mathematical model and the force-acceleration mechanical transfer function, the effectiveness of the mathematical model is completely and successfully verified.

As an example Fig. 4 and 5 report the simulated (dotted line) and the measured (continuous line) axial vibration spectra of the motor working respectively at full load with a broken bar and at 75% load with a bar cracked for 75% of its depth.

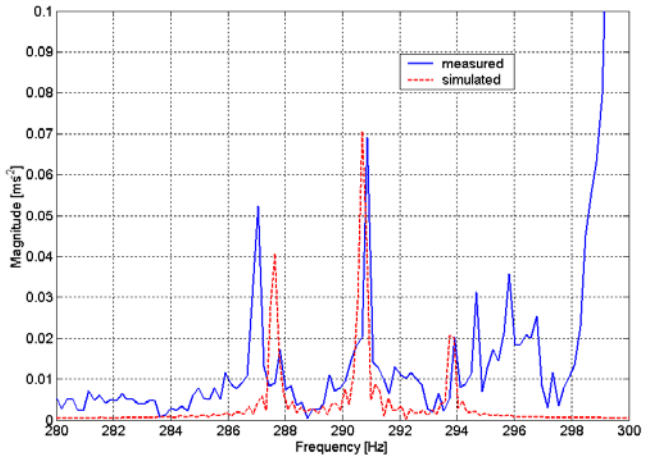

Fig. 4. Simulated and measured axial vibration spectra at full load and with a broken rotor bar.

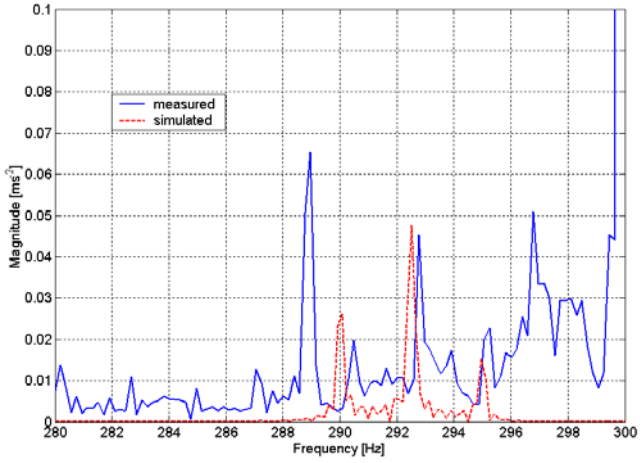

Fig. 5. Simulated and measured axial vibration spectra at 75% of full load and a cracked bar for 75% of its cross section

The small frequency shift is due to the error in slip measurement, but, in any case, this circumstance does not compromise the fault detection.

3. DIAGNOSIS TECHNIQUE

After the validation of the proposed mathematical model, we performed several simulations varying the motor loads and the degrees of fault.

The analysis of both the simulations and the experimental tests results shows that, when a fault condition occurs, the higher amplitude frequency components are the three near 6*f* (in our case 300 Hz).

Fig. 6 shows the frequencies of the three fault components (the ones related to 6*f*) of axial vibration as a function of the motor slip.

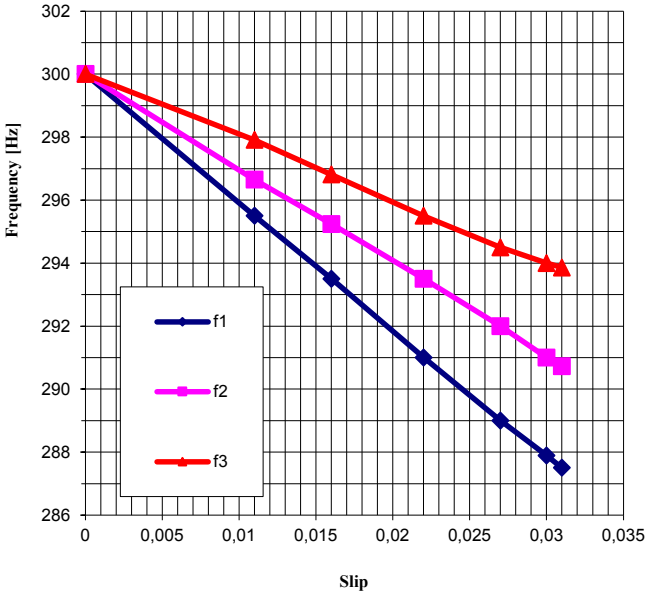

Fig. 6. Frequencies of the fault components versus the motor slip

It is possible to notice that the frequency of the three components is linearly depending on the slip. In particular, the lower is the slip, the nearer is the fault components to the harmonic component (300 Hz in our case).

This circumstance makes difficult the fault detection when the motor is without mechanical load and requires a better frequency resolution in the frequency analysis.

As fault index, we chose the average value (A) of the amplitude of these components, given that it raises when the entity of fault increase.

In particular, we evaluated A for four defined fault conditions of the rotor bar, and so, for four defined percentage of the bar crack; namely 25 % (A_1), 50 % (A_2), 75 % (A_3) and 100 % (A_4).

Fig. 7 shows the trends of the average amplitudes of the three fault components of the axial vibration versus the bar fault entity with the motor slip as parameter.

It is possible to notice that the amplitudes of these components depend not only on the entity of the crack of the rotor bar, but also on the slip. This circumstance requires that, for a correct diagnosis, the slip or the angular velocity of the rotor must be known or measured.

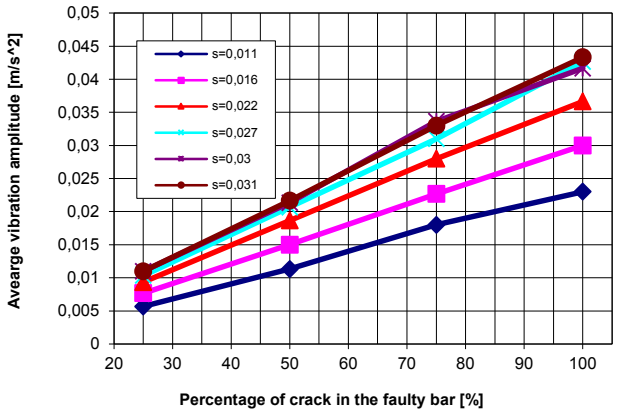

Fig. 7. Average amplitude A of fault components versus percentage of crack in the faulty bar with the motor slip as parameter

The values A_1, A_2, A_3 and A_4 are chosen as limits of five regions that individuate the entity of the fault:

1. quasi healthy bar if $0 \le A < A_1$
2. slightly cracked bar if $A_1 \le A < A_2$
3. medium cracked bar if $A_2 \le A < A_3$
4. heavy cracked bar if $A_3 \le A < A_4$
5. broken bar if $A \ge A_4$

Obviously, it is necessary to take into account that the fault components amplitude depends also on the motor slip and, therefore, it is necessary to calculate A_1, A_2, A_3, and A_4 for various slip values.

Fig. 8 shows the trends of the average amplitudes of the three fault components of the axial vibration versus the motor slip for each faulty condition considered. These curves distinguish five regions of the A-s plane each of those individuate the fault entity. Therefore, the coordinates of the four curve points, stored in a look-up table, can be used to implement a diagnostic system based on the axial vibration monitoring.

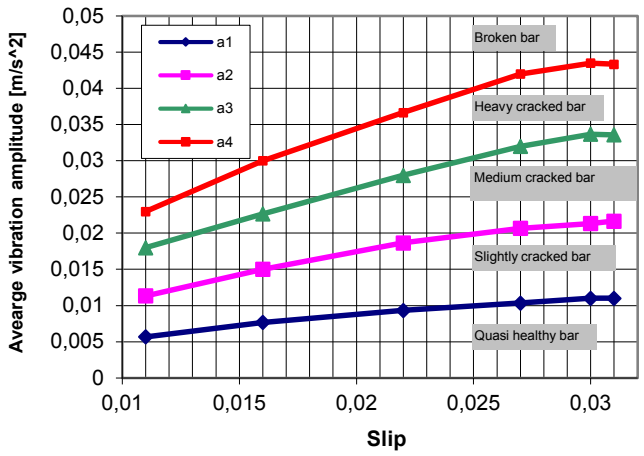

Fig. 8. Average amplitude A of fault components versus motor slip with the percentage of crack as parameter.

3. CONCLUSIONS

In the paper, we presented a method to detect cracks on the rotor bars of the squirrel cage motors. The approach is based on the analysis of the axial vibration spectrum and on a mathematical model, which allows relating the vibrations to the entity of the faults. In order to validate the proposed model, we performed various experimental tests, under different mechanical load conditions both in healthy and faulty motors.

Eventually, we propose a fault index, easily obtainable from the axial vibration spectrum. By means of this index, it is possible not only detect the faults, but also evaluate the severity degree of the faults.

In order to make cheaper the implementation of the diagnostic technique, we are carrying out other tests, using, instead of the Brüel & Kjær accelerometer, some not-conventional acceleration sensors (such as buzzers, microphones and pickups).

ACKNOWLEDGMENTS

This publication was partially supported by the PON04a2_H "i-NEXT"" Italian research programs. This work was realized with SDESLab - University of Palermo.

REFERENCES

[1] A.H. Bonnett and C. Yung, "Increased Efficiency Versus Increased Reliability", *IEEE Industry Applications Magazine*, Vol. 14 No 1, 2008, pp. 29-36.

[2] S. Ferkolj and R. Fiser "On Line Fault Diagnostic Techniques of Induction Motor Drive", *IEEE/KTH Stockholm Power Tech Conference,* Stockholm, Sweden, pp. 162-166, 18-22 June 1985.

[3] A. Stefani, A. Yazidi, C. Rossi,, F. Filippetti, D. Casadei and G. A. Capolino, "Doubly Fed Induction Machines Diagnosis Based on Signature Analysis of Rotor Modulating Signals", *IEEE Transactions on Industry Applications*, Vol. 36 No 6, 2008, pp. 1717-1721.

[4] Kerszenbaum and Landy, "The Existence of Large Inter-bar Currents in Three Phase Cage Motors with Rotor-bar and /or End-ring Faults", *IEEE Transactions on Power Apparatus and Systems*, Vol. PAS-103, no.7, pp. 1854-1862, July 1984.

[5] R.F.Walliserand and C.F. Landy, "Assessment of interbar currents in double cage induction motors with broken bars ", *IEEE Transactions on Energy Conversion*, Vol. 9 No. 1, 1994, pp.159-164.

[6] H. Müller and C.F. Landy, "Finite Element Analysis of Field Distribution of Squirrel Cage Induction Motors Having Broken Rotor Bars and Interbar Currents", *Proceedings of ICEM, International Conference on Electrical Machines*, pp. 577-581, Paris, France, 5-8 September 1994.

[7] H. Müller and C.F. Landy, "Vibration Produced in Squirrel Cage Induction Motors Having Broken Rotor Bars and Interbar Currents", *Proceedings of ICEM, International Conference on Electrical Machines*, pp. 595-600, Paris, France, 5-8 September 1994.

[8] A. O. Di Tommaso and R. Miceli, "A Mathematical Model and Test Bench for Vibration Spectral Analysis to Detect a Broken Bar in Squirrel Cage Induction Motors", *Proc. of SDEMPED 2001 Symposium,* pp. 617-622, Grado, Italy, September 2001.